



**HAL**  
open science

# Flocculation-flotation harvesting mechanism of *Dunaliella salina*: From nanoscale interpretation to industrial optimization

Alexandre Besson, Cécile Formosa-Dague, Pascal Guiraud

► **To cite this version:**

Alexandre Besson, Cécile Formosa-Dague, Pascal Guiraud. Flocculation-flotation harvesting mechanism of *Dunaliella salina*: From nanoscale interpretation to industrial optimization. *Water Research*, 2019, 155, pp.352-361. 10.1016/j.watres.2019.02.043 . hal-02618577

**HAL Id: hal-02618577**

**<https://hal.inrae.fr/hal-02618577>**

Submitted on 22 Oct 2021

**HAL** is a multi-disciplinary open access archive for the deposit and dissemination of scientific research documents, whether they are published or not. The documents may come from teaching and research institutions in France or abroad, or from public or private research centers.

L'archive ouverte pluridisciplinaire **HAL**, est destinée au dépôt et à la diffusion de documents scientifiques de niveau recherche, publiés ou non, émanant des établissements d'enseignement et de recherche français ou étrangers, des laboratoires publics ou privés.



Distributed under a Creative Commons Attribution - NonCommercial 4.0 International License

1 **Flocculation-flotation harvesting mechanism of *Dunaliella salina*: from nanoscale**  
2 **interpretation to industrial optimization**

3 Alexandre Besson<sup>1\*</sup>, Cécile Formosa-Dague<sup>1,2,3\*</sup> and Pascal Guiraud<sup>1,3</sup>

4

5 <sup>1</sup> LISBP, Université de Toulouse, INSA, INRA, CNRS, Toulouse, France

6 <sup>2</sup> LAAS, Université de Toulouse, CNRS, Toulouse, France

7 <sup>3</sup> Fédération de recherche FERMAT, CNRS, Toulouse, France

8

9

10 Corresponding author: Prof. Pascal Guiraud, [pguiraud@insa-toulouse.fr](mailto:pguiraud@insa-toulouse.fr)

11 \*These two authors equally contributed to the work

12

13

14

15 **Abstract**

16 *Dunaliella salina* is a green microalgae species industrially exploited for its capacity to produce  
17 important amounts of carotenoid pigments. However in low nitrogen conditions in which they  
18 produce these pigments, their concentration is low, which results in harvesting difficulties and high  
19 costs. In this work, we propose a new solution to efficiently harvest *D. salina* at the pre-industrial  
20 scale, using flocculation/flotation harvesting induced by NaOH addition in the medium. We first  
21 show, using numerical simulations and nanoscale atomic force spectroscopy experiments, that  
22 sweeping mechanism in formed magnesium hydroxide precipitate is only responsible for *D. salina*  
23 flocculation in hypersaline culture medium upon NaOH addition. Based on this understanding of the  
24 flocculation mechanism, we then evaluate the influence of several parameters related to NaOH  
25 mixing and magnesium hydroxide precipitation and show that NaOH concentration, mixing, and  
26 salinity of the medium can be optimized to achieve high flocculation/flotation harvesting efficiencies  
27 in laboratory-scale experiments. We finally successfully scale-up the data obtained at lab-scale to a  
28 continuous pre-industrial flotation pilot, and achieve up to 80% of cell recovery. This interdisciplinary  
29 study thus provides original results, from the nano- to the pre-industrial scale, which allow the  
30 successful development of an efficient large-scale *D. salina* harvesting process. We thus anticipate  
31 our results to be the starting point for further optimization and industrial use of this  
32 flocculation/flotation harvesting technique.

33

34

35

36

37

38

39

40

41 **Keywords**

42 *Dunaliella salina*, Harvesting, Flocculation, Flotation, Atomic force microscopy

## 43 1. Introduction

44 Microalgae are receiving increasing attention worldwide as an alternative and renewable  
45 source of energy because of their eminent oil producing capacity (Pragya et al., 2013). But the  
46 potential of microalgae is in fact even greater and they also represent an important source of  
47 biomass and of molecules of interest for the fields of food, feed or health. Indeed, microalgae are  
48 unique microorganisms which convert light energy, water and inorganic nutrients into biomass  
49 resource rich in value-added products such as lipids, carbohydrates, proteins and pigments (Minhas  
50 et al., 2016; Pragya et al., 2013). Among the wide diversity of microalgae (Metting, 1996), *Dunaliella*  
51 *salina*, a halotolerant green microalgae, is among the species currently industrially exploited, as it is  
52 one of the most important producer of natural  $\beta$ -carotene pigments (Pirwitz et al., 2015; Ambati et  
53 al., 2018). Because of this specificity, *D. salina* has been the subject of many studies dedicated to the  
54 optimization of its culture conditions (Prieto et al., 2011; Kim et al., 2012; Khadim et al., 2018; Béchet  
55 et al., 2018) and of its harvesting (Besson and Guiraud, 2013; Pirwitz et al., 2015; Xiong et al., 2015).  
56 Moreover, other studies have showed the utility of this microalgae species in genetic and metabolic  
57 engineering (Feng et al., 2014; Anila et al., 2016), and also recently in concrete biomedical  
58 applications, for example to reduce tumor growth in mice (Srinivasan et al., 2017).

59 However, under  $\beta$ -carotene production culture conditions (nitrogen deficiency conditions), *D.*  
60 *salina* reaches low cell concentrations which thus has consequences on the energy input and overall  
61 cost of their separation from water in industrial processes. In a general manner, several methods can  
62 be used for microalgae harvesting, including centrifugation, filtration, flocculation and flotation (Garg  
63 et al., 2012). However, most of these methods are synonymous with high costs and energy  
64 consumption, often for low efficiency rates. For example, centrifugation, the most commonly used  
65 method, consumes a large amount of energy and can cause damages to the cells because of high  
66 shear forces (Pragya et al., 2013). Filtration involves using membranes, which, in the case of  
67 microalgae separation, can get clogged because of the small size of the cells and/or of the  
68 exopolysaccharides they secrete, resulting in high operating costs (Uduman et al., 2010). As for

69 flocculation, it seems to be a promising low-cost approach for large-scale harvesting; however,  
70 contamination is a major issue in this technique, as the chemical flocculants classically used to induce  
71 flocculation end up in the harvested biomass, and can interfere with the final application of the  
72 biomass (food or feed) (Vandamme et al., 2013).

73 In this context, flotation is believed to be a promising harvesting technique that takes  
74 advantage of microalgae's natural low density and self-floating tendency (Garg et al., 2012). Assisted  
75 flotation consists in air or gas transformed into bubbles rising through a microalgae suspension. As a  
76 result, microalgae cells get attached to bubbles and are carried out and accumulated on the surface.  
77 Thus flotation allows for low-cost cell harvesting, without necessarily using flocculants that could  
78 damage the cells. In addition, it is a relatively rapid operation, which needs low space and has  
79 moderate operational costs. However, as both the surface of microalgae and bubbles present a  
80 negative charge in aqueous medium (Yang et al., 2001; Garg et al., 2015), and given the low  
81 hydrophobicity of microalgae cells, the interactions between cells and bubbles are repulsive, which  
82 prevents adhesion, and thus capture and flotation, resulting in the poor efficiency of this harvesting  
83 technique.

84 Among the possible strategies to enhance flotation efficiency, natural auto-flocculation is an  
85 interesting alternative. There are several known auto-flocculation mechanisms, among which one is  
86 based on the precipitation of magnesium ions into magnesium hydroxide at high pH (Sukenik and  
87 Shelef, 1984). Such increased pH in the culture medium can result either from the photosynthesis  
88 activity of the cells or from the direct addition of  $\text{OH}^-$ . Then the flocculation of the cells can occur  
89 through charge neutralization, *i.e.* through the interaction between the positively charged formed  
90 magnesium hydroxide precipitates and cells, through sweeping where cells are entrapped in the  
91 massive precipitation of the magnesium hydroxide in the medium, or both (Vandamme et al., 2013).  
92 Auto-flocculation of cells at high pH using NaOH addition has already been described for different  
93 microalgae species, such as *Chlorella vulgaris* (Wu et al., 2012), or *Phaeodactylum tricoratum* (Wu  
94 et al., 2012; Vandamme et al., 2015; Formosa-Dague et al., 2018) and has been showed to occur by

95 both sweeping flocculation and charge neutralization. In the case of *D. salina*, a previous study that  
96 we conducted in 2013 showed that addition of NaOH was necessary to increase the pH in the  
97 medium, and that further flocculation was caused by sweeping of the cells by forming magnesium  
98 hydroxide precipitate (Besson and Guiraud, 2013). In the experimental conditions used in this study,  
99 the more NaOH was added, the more magnesium hydroxide was precipitated and the more efficient  
100 the flocculation was; a cell recovery up to 100% could be achieved using further flotation. The results  
101 obtained also showed that the NaOH flow rate had no influence on the flocculation and further  
102 flotation recovery; however they suggested that the type of injection of NaOH, and thus its mixing in  
103 the medium and the speed of magnesium hydroxide precipitation, could have an influence in the  
104 final harvesting efficiency.

105 In the work presented here, we will first evidence the only contribution of sweeping  
106 mechanism in the flocculation of cells induced by the precipitation of magnesium hydroxide at high  
107 pH, and exclude the role of charge neutralization. For that we will first simulate the precipitation of  
108 magnesium hydroxide in the medium as a function of the NaOH concentration to understand the  
109 behavior of the culture medium during flocculation. Then, we will use recent developments made in  
110 the team that consist in using atomic force microscopy (AFM) (Binnig et al., 1986) to probe the  
111 interactions between microalgae cells and particles (Formosa-Dague et al., 2018). For that, AFM tips  
112 functionalized with magnesium hydroxides particles will be used in force spectroscopy experiments  
113 to measure directly, at the piconewton scale, the interactions between these particles and the cells.  
114 Then, knowing precisely the flocculation mechanism at play, we will be able to optimize parameters  
115 to harvest, in the most effective possible way, *D. salina* cells at laboratory scale but also at pre-  
116 industrial scales (suspension flow rate  $0.6 \text{ m}^3/\text{h}$ ). For that, we will complete our previous study and  
117 determine the role of NaOH mixing in the medium by testing different injection types, agitation and  
118 medium salinity, and by evaluating their effects on the flocculation/flotation recovery of the cells at  
119 laboratory scale. Based on these results and their interpretation, we will adapt and optimize an  
120 injection system to efficiently flocculate and harvest cells by flotation in a pre-industrial continuous

121 cultivation system. This way we will provide a cost-effective solution to efficiently harvest low-  
122 concentrated *D. salina* cells at industrial scales, thus contributing to the industrial valorization of this  
123  $\beta$ -carotene rich biomass.

124

## 125 **2. Material and methods**

### 126 **2.1. Strain and culture conditions**

127 *Dunaliella salina* strain CCAP19/25 (Culture Collection of Algae and Protozoa) was cultivated in  
128 dechlorinated tap water containing the following: NaCl (107 g/L); MgSO<sub>4</sub>.7H<sub>2</sub>O (4.8 g/L); MgCl<sub>2</sub>.6H<sub>2</sub>O  
129 (4.0 g/L); CaCl<sub>2</sub> (1.1 g/L); KCl (0.1 g/L). A complete nutritive Conway medium (without silicates)  
130 (Walne, 1970) was also added. The salinity of this synthetic water is of 10%, the ionic strength of 2.3.  
131 This medium was used for all the experiments performed in laboratory. It mimics the medium  
132 resulting from the evaporation of sea water in which *D. salina* can grow with a limited competition  
133 from other microorganisms, used in pre-industrial scale cultures. A *D. salina* strain isolated from  
134 saline ponds in Gruissan, Occitanie, France, was also used to evaluate the influence of the strain on  
135 the harvesting efficiencies.

136 Laboratory-scale cultures: For AFM experiments, cells were cultivated at 20°C, under agitation (120  
137 rpm), in 75 mL non-coated culture flasks (15 mL of culture), 500 mL non-coated culture flasks (150  
138 mL of culture). The incubator was equipped with white neon light tubes providing illumination of  
139 approximately 40  $\mu\text{mol photons m}^{-2} \text{s}^{-1}$  with a photoperiod of 12h light : 12h dark. For flotation  
140 experiments, *D. salina* culture was achieved in 10 L glass photobioreactors. The culture was  
141 continuously agitated by the gentle bubbling of 0.2  $\mu\text{m}$  filtered atmospheric air (2 L/min).  
142 Illumination was provided by daylight fluorescent tubes (OSRAM FQ 965 Biolux) with a photoperiod  
143 of 16h light : 8h dark. The temperature of the culture was regulated by air conditioning at  $21 \pm 3^\circ\text{C}$ .

144 Pre-industrial scale cultures: The pre-industrial experimental site of the Salinalgue research project  
145 (2010-2014) was located in a salt marsh on the Mediterranean Sea coast, at Gruissan, Occitanie,  
146 France (Latitude: 43.094 N; Longitude: 3.084 E), as fully described in Béchet *et al.* (Béchet *et al.*,

147 2018). Briefly, cultures were achieved in 4 outdoor raceways of 250 m<sup>2</sup>, containing between 30 and  
148 100 m<sup>3</sup>. See water concentrated by sun evaporation (salinity of 12%) and disinfected with bleach fed  
149 the raceways before being inoculated. The raceways were mixed by paddle wheels and by  
150 suspension pumping which was also used to limit the pH to 7.4 by a monitored addition of dissolved  
151 CO<sub>2</sub> in the recirculated suspension.

152

## 153 **2.2. Precipitation model for hydroxide magnesium in the culture medium used**

154 The concentration of magnesium hydroxide, calcium carbonate and dolomite were modeled as a  
155 function of the added NaOH concentration in the culture medium. To do so, we simulated the NaOH  
156 addition effects and developed a numerical model, using the software Phreeqc, based on the Pitzer  
157 equations to simulate the precipitate formation in our culture medium. Indeed, in order to assess the  
158 equilibrium state of hypersaline solutions in which *D. salina* is grown and understand the  
159 precipitation phenomena involved during NaOH addition, it is necessary to evaluate the activity of  
160 species in solution. This requires the evaluation of coefficients of activity, which take into account the  
161 various ionic interactions in these complex environments. The models for calculating these activity  
162 coefficients are generally based on the coupling of the Debye-Hückel (Debye and Hückel, 1923)  
163 theory translating electrostatic ionic interactions, and of the theory of the ionic association that takes  
164 into account ionic interactions at short distances. These models are well suited for solutions with  
165 ionic strength that does not exceed the one of regular seawater (ionic strength of 0.7). But since the  
166 culture of *D. salina* is carried out in a hypersaline environment, the ionic forces encountered in its  
167 culture medium exceed the areas of validity of the different ion association models (for a 10% salinity  
168 culture medium, the ionic strength is of 2.3). Therefore, the models obtained with these theoretical  
169 descriptions of saltwater thermodynamics are not satisfactory for concentrated saline water. In the  
170 case of *D. salina*, it was thus necessary to implement other types of models, known as specific ion  
171 interaction models, such as the one proposed by Pitzer. The Pitzer model is based on a different  
172 thermodynamic approach, and is well suited to evaluate the thermodynamic properties of



173 hypersaline solutions. The model used is based on the Pitzer equations, and allows to simulate the  
174 ionic equilibria during the injection of NaOH in our culture medium. The models developed by Pitzer  
175 (Pitzer, 1973; Pitzer and Mayorga, 1973, 1974; Pitzer and Kim, 1974; Pitzer, 1975) describes the  
176 specific ionic interactions of diverse species in complex media, at high ionic strength. For pure  
177 components, this model uses the parameters given by (Pitzer and Mayorga, 1973, 1974). The  
178 asymmetric mixing parameters come from Pitzer ~~et~~ and Kim (Pitzer and Kim, 1974; Pitzer, 1975). The  
179 whole set of parameters were validated and listed by Harvie *et al.* (Harvie et al., 1984), the relevant  
180 database being “pitzer.dat” This database accounts for the significant elements for Mediterranean  
181 sea water (Na-K-Mg-Ca-H-Cl-S-O-C-Fe-Mn-Ba-Sr-B-Li-Br) with a large spectrum of possible  
182 precipitates. Before its application for the simulations presented here, the model has been  
183 successfully (Besson, 2013) compared to the experimental results of sea water evaporation proposed  
184 by Baseggio (Baseggio, 1974). The composition of the culture medium used for the simulations (Table  
185 1) was entered using a temperature of 25°C and a total dissolved carbon concentration of 0.00021  
186 mol/kg\_water.

187 **Table 1.** Concentrations of the main ions in the culture medium used in simulations in g/L

Na <sup>+</sup>	Cl <sup>-</sup>	SO <sub>4</sub> <sup>2-</sup>	Mg <sup>2+</sup>	Ca <sup>2+</sup>	K <sup>+</sup>
42.12	67.08	1.87	0.95	0.39	0.04

188

### 189 **2.3. Flotation experiments**

190 Due to the small size of the microalgae, Dissolved Air Flotation (DAF) was used to harvest *D. salina*  
191 after NaOH-induced flocculation. Figure 1 presents the DAF devices used in this study.

192 Laboratory scale: A detailed presentation of the laboratory scale flotation experiments can be found  
193 in Besson & Guiraud (Besson and Guiraud, 2013). DAF experiments were performed in a Multiplace  
194 Orchidis™ FTH3 Flottatest. Three flotation-test beakers were run simultaneously, in which 600 mL  
195 samples were collected from the algal culture and added to each beaker. Then NaOH was added: in  
196 the case of direct NaOH injection, x mL of NaOH at a concentration of 1M was added to the  
197 microalgae suspension, as well as 100 - x mL of distilled water. In the case of the diluted NaOH

198 injection, a unique solution containing  $x$  mL of NaOH at a concentration of 1M and  $100 - x$  mL of  
199 distilled water was added to the microalgae suspension. The volume of NaOH ( $x$ ) added was  
200 calculated depending on the final concentration wanted. This procedure is presented in figure 4a.  
201 The depressurization at atmospheric pressure of 200 mL culture medium free of algae and saturated  
202 by air at 6 bars for 15 min induced the formation of microbubbles. The recycle ratio (pressurized  
203 culture medium volume/initial sample volume) was of 33%. For flocculation, the concentration of the  
204 added NaOH solution was calculated taking into account the volume of the culture and the volume of  
205 the added white water, so that the pH does not change upon addition of the white waters.

206 Pre-industrial scale: The pre-industrial DAF system was adapted from the CY1 flotation unit proposed  
207 by Sérinol (Bram, Occitanie, France), and is presented in Figure 1. Built in 316L stainless steel to avoid  
208 corrosion by suspensions at high salinity, this continuous cylindrical (0.6 m of diameter) DAF  
209 separation equipment, with a conical bottom, works as an airlift. A cylindrical Clifford delimits the  
210 ascending contact zone where the suspension to be treated and the white waters, containing  
211 bubbles, mix. At the periphery, the descending annular separation zone is equipped with a vertical  
212 lamellar packing to keep the flow as quiet as possible. The nominal descending flow velocity is of 4.0  
213 m/h. The flotation tank volume is of 600 L and its maximum flow capacity is of  $1 \text{ m}^3/\text{h}$ . The floated  
214 microalgae are mechanically removed from the tank surface by a tunable rotating scrapper. Salted  
215 waters identical to the culture medium or recycled from the harvesting are continuously pressurized  
216 at 6 bars by a centrifugal pump and saturated with air within a pressurization tank. White waters are  
217 produced by passing this pressurized solution through a needle valve. The microbubble size  
218 distribution was measured by Laser Diffraction Sizer (Malvern Spraytec): most of the bubbles  
219 produced in these saline waters have a diameter smaller than  $60 \mu\text{m}$  (Besson and Guiraud, 2012).  
220 NaOH solutions at different concentrations in distilled water were added at different injection places  
221 on the supply line at a controlled flow injection using a peristaltic pump. Given that the microalgae  
222 suspension flow rate is of 300 L/h, and the final NaOH concentration is of 0.02 mol/L, if a NaOH  
223 solution of 0.1 mol/L is injected, the flowrate is of 66 L/h, and if a NaOH solution of 0.2 mol/L is

224 injected, the flowrate is of 0.33 L/h. Flowrates were measured thanks to Khrono Optif lux – 4100  
225 electromagnetic flowmeters. For the operating conditions, microalgae suspensions were extracted  
226 from the external raceways using a peristaltic pump, into the flotation unit. Simultaneously, the  
227 pressurization system was launched and the NaOH solutions were injected on the supply line. The  
228 scrapping of the microalgae started as soon as the pressurization system was launched. After one  
229 hour at constant operating parameters (three times the time of the continuous state settling),  
230 samples required to quantify the separation efficiency (treated suspension) were harvested: the  
231 harvesting efficiency was then measured as described below.

232

#### 233 **2.4. Harvesting efficiency quantification**

234 Harvesting efficiency quantification is based on optical density measurements. The harvesting  
235 efficiency represents the quantity of algae floated compared to the quantity in the initial suspension:  
236 it was evaluated using the following equation:

$$E(\%) = \left(1 - \frac{ODaVa}{ODiVi}\right) \times 100$$

237 Where  $ODi$  and  $Vi$  are the initial optical density at 800 nm and the volume of algal suspension before  
238 NaOH addition and flotation,  $ODa$  and  $Va$  are the optical density at 800 nm of the aqueous phase and  
239 the volume of the aqueous phase after injection of pressurized water.

240

#### 241 **2.5. Zeta potential measurements**

242 The global electrical properties of *D. salina* cell surface were assessed by measuring the  
243 electrophoretic mobility which corresponds to the velocity of suspended cells exposed to an electric  
244 field. To this end, microalgae were harvested by centrifugation (1500 rpm, 3 min), washed two times  
245 in sorbitol buffer 375 mM at pH = 10 and resuspended in the same buffer at a final concentration of  
246  $1.5 \times 10^6$  cell/mL. Using this procedure, electrolytes present in the culture medium do not interfere  
247 and only the surface charge of the cells is measured. The electrophoretic mobility was then

248 measured using an automated laser zetameter (Zetasizer NanoZS, Malvern Instruments). Cell  
249 suspensions coming from 2 independent cultures were analyzed.

250

251

252

## 253 **2.6. AFM tip functionalization with hydroxides**

254 To prepare functionalized AFM with  $\text{Mg}(\text{OH})_2$ , MLCT AUWH tips were first dipped into a thin layer of  
255 UV-curable glue (NOA63, Norland Edmund Optics), then into a thin layer of  $\text{Mg}(\text{OH})_2$  particles (Sigma-  
256 Aldrich) deposited on a glass slide. Functionalized tips were then put under UV-light for 10 min to  
257 allow the glue to cure.

258

## 259 **2.7. AFM imaging and force spectroscopy experiments**

260 Before AFM experiments, cells were harvested by centrifugation (3000 rpm, 10 min) and washed two  
261 times in sorbitol buffer 375 mM at pH = 10. This salt-free buffer is used for force spectroscopy  
262 experiments as it allows to accurately measure interactions between the cells and magnesium  
263 hydroxide particles functionalized on the AFM tips without introducing a bias from electrolytes  
264 present in *D. salina* culture medium. Moreover, the sorbitol present in this buffer keeps the cells  
265 from exploding because of the osmotic pressure. Finally, the pH of 10 allows to reproduce the  
266 conditions in which the cells are during flocculation induced by addition of NaOH. Cells were then  
267 immobilized on polyethylenimine (PEI, Sigma P3143) coated glass slide prepared as previously  
268 described (Francius et al., 2008). Briefly, freshly oxygen activated glass slides were covered by a 0.2%  
269 PEI solution in deionized water and left for incubation overnight. Then the glass slides were rinsed  
270 with deionized water and dried under nitrogen. A total of 1 mL of cell suspension was then deposited  
271 on the PEI slides, allowed to stand for 30 min at room temperature, and rinsed with sorbitol buffer  
272 375 mM at pH = 10. For force spectroscopy experiments, MLCT AUWH cantilevers with a nominal  
273 spring constant of 0.01 N/m, functionalized with hydroxides or not, were used at a constant applied

274 force of 0.25 nN. The cantilevers spring constants were determined using the thermal noise method  
275 (Hutter and Bechhoefer, 1993) before each experiment.

276

277

278

### 279 **3. Results and discussion**

#### 280 **3.1. Precipitation modeling and AFM force spectroscopy confirm that *D. salina* is flocculated by** 281 **sweeping in magnesium hydroxide precipitate at high pH**

282 In our previous study in 2013 (Besson and Guiraud, 2013), our work evidenced the positive  
283 effect of NaOH addition on the flocculation of *D. salina*. Our main results showed indeed an increase  
284 in the harvesting efficiency with the addition of NaOH into the medium, up to 80% of cell recovery.  
285 While the hypothesis that the flocculation occurred through sweeping in magnesium hydroxide  
286 precipitate could be formulated, notably thanks to ions chromatography experiments performed on  
287 the suspension before and after flocculation/flotation, no proof of this mechanism were brought.  
288 The first part of this study thus focus on providing a full understanding of the NaOH-induced  
289 flocculation mechanism. For that we first assessed the equilibrium state of the hypersaline solutions  
290 in which *D. salina* is grown to understand the precipitation phenomena involved when flocculating  
291 this microalgae using NaOH addition. For that, we used the model described in section 2.2,  
292 elaborated from the Pitzer model, to successfully simulate the influence of the addition of NaOH on  
293 the ionic equilibria in our culture medium described in Table 1. Results are presented in Figure 2: on  
294 this graph, the precipitation of magnesium hydroxide  $Mg(OH)_2$  is plotted as a function of the added  
295 NaOH concentration. The resulting pH as well as two other precipitate candidate concentrations are  
296 also presented. Even if the measure of pH in hypersaline solutions with a high ionic strength presents  
297 some problems, the simulated pH profile is similar to experimental measurements, as the one  
298 showed in our previous study (Besson and Guiraud, 2013). The pH sharply increases until the  
299 beginning of the precipitation of the magnesium hydroxide. Then, it continues to slightly increase

300 until the end of the  $\text{Mg}(\text{OH})_2$  precipitation, that is to say when all the Mg present in the solution is  
301 used. Thus this shows that upon addition of NaOH, magnesium hydroxide precipitation increases  
302 until reaching a maximum for a NaOH concentration between 0.08 and 0.1 mol/kg of water, while  
303 calcium carbonates precipitation remains non-significant. Thus we can conclude from this simulation  
304 that the hypothesis made in our previous study, stating that flocculation of *D. salina* at increased pH,  
305 under hypersaline conditions at least, results from the precipitation of only magnesium hydroxide at  
306 high pH, among a great number of other possible salts, is correct. While this precipitation creates a  
307 gel that entraps the cells and flocculate them through sweeping, the question is now to know if  
308 charge neutralization is also involved in this flocculation mechanism, thus to have a full  
309 understanding of it.

310 To answer this question we used AFM and performed force spectroscopy experiments using  
311 functionalized tips with magnesium hydroxides particles. In this type of experiments, the AFM tip is  
312 moved towards the surface until touching it, and then retracted. If an interaction takes place  
313 between the tip and the sample, upon retraction, the tip will bend until the force applied is higher  
314 than the force of the interaction and the interaction breaks. The tip then goes back to its initial  
315 position, which is materialized on AFM retract force curves as a peak, referred to as retract adhesion.  
316 The results of these experiments are presented in figure 3, they show in the case of bare AFM tips no  
317 adhesion between the tip and the cells, as seen on the retract force curves which present no retract  
318 adhesions (Figure 3a and b, n=2400 curves recorded on 6 cells from 2 independent cultures). In the  
319 case of tips functionalized by magnesium hydroxides (Figure 3C and d), force curves also show no  
320 retract adhesions, thus demonstrating that hydroxide particles do not interact with cells (n=3200  
321 curves recorded on 8 cells coming from 2 independent cultures, with 7 different  $\text{Mg}(\text{OH})_2$  tips). Note  
322 that in order to avoid any interaction between electrolytes in the medium and the AFM tips,  
323 experiments were performed in a salt-free buffer at pH=10 to make sure only the interactions  
324 between the cells and the tips are probed. As no interactions were probed in this buffer, it is then  
325 evident that in the hypersaline waters in which *D. salina* grows, these interactions do not occur

326 neither given the high quantity of charged ions that can screen both cells and  $\text{Mg}(\text{OH})_2$  particles  
327 charges. To give an explanation to this absence of interactions between the cells and  $\text{Mg}(\text{OH})_2$   
328 particles, we then performed zeta potential measurements of *D. salina* cells in the same salt-free  
329 buffer at high pH (pH = 10), and measured a surface charge of  $-15.4 \pm 0.9$  mV (n=8 measurements on  
330 cell suspensions coming from 2 independent cultures). Thus the cells do not present a sufficient  
331 negative surface charge in our conditions, and do not interact with the positive surface of  
332 magnesium hydroxide (Lin and Wang, 2009).

333 Therefore thanks to these simulations and AFM experiments, we are able to confirm the  
334 hypothesis we made in our previous study, and show that addition of NaOH in the culture medium  
335 precipitates only magnesium hydroxide. This precipitation results in the formation of a gel that is  
336 only responsible for entrapping the cells and flocculating them, as AFM experiments proved that  
337 charge neutralization is not involved in the case of *D. salina*. Moreover, in further experiments that  
338 we performed,  $\text{Mg}(\text{OH})_2$  already formed was directly added to *D. salina* cultures, which resulted in no  
339 flocculation of the cells, thus reinforcing our nanoscale conclusions. This is an interesting point as for  
340 all the microalgae species for which pH-induced flocculation has been described, charge  
341 neutralization mechanism is always involved (Sukenik and Shelef, 1984; Wu et al., 2012; Vandamme  
342 et al., 2012; Nguyen et al., 2014; Vandamme et al., 2015; Formosa-Dague et al., 2018; Branyikova et  
343 al., 2018). Indeed, microalgae often have a cell wall, composed of lipids, proteins and  
344 polysaccharides. These last ones have a  $\text{pK}_a$  of 11-12; when the pH increases in the medium, the  
345 hydroxyl functions of these polysaccharides are deprotonated, which can give the surface a more  
346 important negative charge. As microalgae are usually grown in waters containing calcium or  
347 magnesium ions, which precipitate into positively charged particles at high pH, then flocculation  
348 occur also thanks to the interaction between these particles and the cells. However in our case, *D.*  
349 *salina* cells do not interact with positively charged magnesium hydroxide. Indeed, *Dunaliella* genus is  
350 unique in the absence of a rigid polysaccharidic cell wall; cells only present a thin plasma membrane  
351 (Oren, 2005; Chen and Jiang, 2009). This thus explains why its surface charge is not more negative at

352 high pH, and thus why charge neutralization is not involved in its flocculation mechanisms in  
353 presence of magnesium hydroxide. Thus our results give a full understanding of the mechanism of *D.*  
354 *salina* flocculation at high pH; based on these information, we can now evaluate the influence of  
355 different parameters, such as NaOH concentration, agitation and salinity in order to determine the  
356 best possible separation conditions of the cells from the water, and provide a solution for high-scale  
357 harvesting.

### 358 **3.2. Magnesium hydroxide precipitation phase is determinant for flocculating the cells**

359 Because the flocculation of the cells occur only through sweeping, the precipitation of  
360 magnesium hydroxide is then determinant for the successful flocculation/flotation of the cells.  
361 Indeed, the precipitation phase must be carried out as homogeneously as possible, so that as much  
362 of the sample volume as possible is affected by the trapping of microalgae in the precipitate in  
363 formation. Therefore, the conditions for adding NaOH to the suspension should be adapted to  
364 optimize its fast mixing. To address this point, we performed flocculation/flotation experiments using  
365 two different injection ways (Figure 4a), reaching the same final NaOH concentration. In the first way  
366 (direct injection), NaOH (1 mol/L) and water are directly injected in a flotation unit containing the  
367 microalgae suspension. In the second way, called here diluted injection, water and NaOH (1 mol/L)  
368 are first mixed into one solution, which is further added to the microalgae suspension. Then, in the  
369 first case, concentrated NaOH is delivered locally into the medium and in the second case, the local  
370 instant concentration of the NaOH solution is reduced. Using these two injection scenarios,  
371 flocculation/flotation harvesting was performed: the results, presented in Figure 4b show a clear  
372 increase of the harvesting efficiency in the case of diluted injection, for the same final NaOH  
373 concentration in the microalgae suspension (black-filled symbols). For example at 0.02 mol/L of final  
374 NaOH concentration, the harvesting efficiency using direct injection is of almost 30% whereas using  
375 the diluted injection system, it reaches up to 90%. Indeed, in the case of direct injection, a high  
376 quantity of concentrated NaOH is locally delivered in the solution, thus the speed of precipitation is  
377 increased but only concerns a local area of the suspension. Therefore in this case, only the cells



378 present in this area can be entrapped during the precipitation of magnesium hydroxide. In the case  
379 of the diluted injection, the low local concentration allows for a slower precipitation, which then has  
380 time to occur in the entire, or at least a larger volume of the microalgae suspension, leading to the  
381 entrapment of more cells. This phenomena is further illustrated in Figure 4c; for a final NaOH  
382 concentration in the microalgae suspension of 0.02 mol/L, the more diluted the added NaOH solution  
383 is, the more efficient the harvesting is. Indeed, for an added NaOH solution of 0.1 mol/L, the  
384 flocculation/flotation cell recovery reaches 80% while for NaOH solutions higher than 0.5 mol/L, the  
385 harvesting efficiency is reduced to 20%.

386         The results of these experiments then prove that the local concentration of NaOH and the  
387 phase of the magnesium hydroxide precipitation is determinant for the harvesting efficiency. While  
388 diluted injection allows lowering this local NaOH concentration, to optimize the conditions to reach  
389 the best cell separation possible, other parameters such as the agitation and the salinity (quantity of  
390 magnesium ions available) of the medium should be taken into account as they will thus also  
391 influence the harvesting efficiency.

392

### 393 **3.3. Agitation and salinity are parameters that influence harvesting efficiency**

394         While diluted injection allows the magnesium hydroxide precipitate to form slowly in the  
395 medium, agitation of the medium allows for the precipitation phase to sweep the entire microalgae  
396 suspension. In Figure 5a, the effects of different agitation speed on the flocculation/flotation  
397 harvesting efficiency were measured. It is clear on this figure that an increase from 20 to 40 rpm  
398 allows increasing by approximately a two-fold the cell separation whatever the final NaOH  
399 concentration in the microalgae suspension. However, increasing again the agitation speed from 40  
400 to 80 rpm do not show the same effect, as the harvesting efficiency in the case of 80 rpm agitation is  
401 slightly lower than in the case of 40 rpm. This can be explained by the fact that a too fast agitation  
402 can change the structure of the flocs formed and thus have consequences on their capture by the  
403 bubbles during flotation. As for the salinity of the medium, to assess its effects on the harvesting

404 efficiency, we performed experiments with *D. salina* cells grown in natural seawaters presenting  
405 salinities of 7.5, 12 and 15.2%, using a dilute injection system and an agitation of 40 rpm. The results  
406 obtained, presented in Figure 5b, show that the more saline the medium is, the less efficient the  
407 harvesting is, whatever the NaOH final concentration. Indeed, while high magnesium concentrations  
408 found in highly saline media can be thought, in the case of sweeping flocculation, to enhance  
409 harvesting efficiency, it is the opposite effect. In high saline media, the NaOH added directly meets  
410 high concentrations of magnesium ions, which induces a fast precipitation of magnesium hydroxide.  
411 OH<sup>-</sup> has thus no time to reach the entire volume of the suspension. Then a high salinity has similar  
412 effects than injection of concentrated NaOH, where only the cells present in the area where fast  
413 precipitation of Mg(OH)<sub>2</sub> occurs can be entrapped in the precipitate, leading to lower separation  
414 rates.

415 Therefore thanks to these experiments, the parameters to reach the best separation rate  
416 possible can be optimized: while a dilute injection is needed, the agitation of the medium must be  
417 optimized to allow an efficient mixing of NaOH with cells and a Mg(OH)<sub>2</sub> precipitation that reaches  
418 the entire volume, without having negative effects on the flocs formed. As for the salinity of the  
419 culture medium, it needs to be low enough to avoid supersaturation of magnesium hydroxide  
420 precipitation, the adequate NaOH concentration depending on the salinity. In order to make sure  
421 that only parameters related to the magnesium hydroxide precipitation have an influence on the  
422 harvesting efficiency, we also evaluated the influence of the calcium concentration, the *D. salina*  
423 strain used, and the nutritive conditions in which the cells are grown. Regarding the influence of the  
424 calcium concentration in the medium, Sukenik *et al.* in 1984 have established that the precipitation  
425 of calcium and phosphate ions at high pH could induce the flocculation of microalgae cells (Sukenik  
426 and Shelef, 1984). The Conway medium used here to cultivate the cells containing phosphate, we  
427 thus used waters of different calcium concentrations to evaluate the potential effect of calcium  
428 phosphate precipitate on the flocculation of *D. salina*. Our results (Supplementary Data 1) showed no  
429 difference in the harvesting efficiencies, thus reinforcing our conclusions on the role of only

430 magnesium hydroxide precipitate in sweeping the cells. The influence of the *D. salina* strain and of its  
431 nutritive conditions have then also been evaluated, and showed that for the two strains we tested  
432 (the CCAP 19/25 and one other *D. salina* strains isolated from saline ponds in France), the same  
433 flocculation/flotation conditions resulted in the same harvesting efficiencies (Supplementary Data 2).  
434 Regarding the nutritive conditions in which cells are grown, we chose to focus on nitrogen deficiency  
435 conditions. Indeed, the overproduction of  $\beta$ -carotene after nitrogen starvation (*i.e.* in conditions of  
436 unbalanced growth in response to lack of nitrogen) is a well-documented biological process in *D.*  
437 *salina* (Lamers et al., 2012; Bonnefond et al., 2017). We thus chose to address this question as the  
438 harvesting method we propose here is intended to be used for industrial use. Our results, with cells  
439 grown in nitrogen deficient conditions, showed no difference in the harvesting efficiencies obtained.  
440 Thus these two last points show that the flocculation/flotation method that we focus on in this study,  
441 when used with the good injection system, agitation and salinity of the medium, is efficient for  
442 different *D. salina* strains, in different relevant culture conditions. This demonstrates the robustness  
443 of this harvesting method, and thus the parameters identified (NaOH injection, agitation and salinity)  
444 can now further be used to develop and adapt a NaOH injection system to efficiently flocculate and  
445 harvest cells by flotation in a pre-industrial continuous cultivation/harvesting system.

446

#### 447 **3.4. Development of a pre-industrial harvesting process of *D. salina* by flocculation/flotation.**

448 In this part of the work, the knowledge previously acquired at the laboratory scale is used to  
449 harvest *D. salina* cells at high-scales. For that, raceways of 250 m<sup>2</sup> were built in Gruissan (Occitanie,  
450 France) and used to cultivate *D. salina*; an industrial continuous flotation unit (600 L) was adapted  
451 and installed on the raceway site to harvest cells using NaOH-induced flocculation/flotation. A  
452 network of pumps with controlled flow rates were used to collect the cells from the raceway and  
453 bring pressurized water into the flotation unit. For adapting the flotation unit to the specific  
454 conditions of *D. salina*, we first faced a technical challenge regarding the size of the bubbles  
455 produced in the pilot. Indeed, using a method based on laser light diffraction, we evaluated the size

456 of the bubbles produced by DAF in *D. salina* culture medium (Supplementary Data 3a). These  
457 experiments show that in this medium (NaCl concentration of 107 g/L), bubbles have a size of  
458 approximately 40  $\mu\text{m}$ , compared to 60-100  $\mu\text{m}$  in freshwater (Edzwald, 1995). Thus the salinity  
459 reduces the size of the bubbles, which results in the reduction of their ascending velocity. While this  
460 is not a problem at small-scale, because the flotation units consist of one small cylinder (1 L of  
461 maximum volume) with only one entry for the pressurized water at the bottom (Figure 1a), at high-  
462 scale in a high-dimensioned flotation unit, presenting descending flow zones, it is a problem. For  
463 instance, this flotation unit presents holes at the base of the Clifford in order to accentuate the airlift  
464 effect and obtain, in nominal functioning conditions, descending speeds of 4 m/h (Figure 1b). We  
465 thus roughly calculated the speed of our bubbles, considering them as rigid particles obeying the  
466 Stokes law corrected by Oseen (Oseen, 1910; Clift et al., 1978) and found in our conditions an  
467 average bubble ascending velocity comprised between 3.6 and 5.4 m/h depending on the  
468 contamination degree of their surface (1 and 1.5 mm/s, Supplementary Data 3b). Thus some of the  
469 bubbles may not reach the surface and can be aspirated in the flow descending zones of the flotation  
470 unit. Thus adaptations directly on the flotation unit were realized, and consisted in decreasing the  
471 surface of the holes present at the base of the Clifford to decrease the airlift effect and decrease the  
472 velocity in these descending flow zones. This way the rising velocity of the microbubbles is higher  
473 than the velocity in the descending flow zones, and thus a functioning similar to what is obtained at  
474 the laboratory-scale can be provided.

475         These adaptations made, we then scaled-up the NaOH-induced flocculation/flotation process  
476 optimized in batch mode at the laboratory scale, to a continuous pre-industrial scale mode. For that,  
477 given the specific flocculation mechanism of *D. salina* by sweeping, it is needed to adapt an injection  
478 system that will ensure a good mixing between the cells and the added NaOH, as it is determinant to  
479 efficiently flocculate the cells. Given the previous results concerning the salinity of the medium,  
480 these experiments were performed in natural seawater at a salinity of 12‰ that ensured the growth  
481 of the cells in the raceway without presenting precipitation supersaturation problems. For the

482 experiments, microalgae cultures were injected into the industrial flotation unit, as well as  
483 pressurized waters, through supply lines following the injection system represented in Figure 6a.  
484 Note that in this system, the waters used for pressurization are recycled from the flotation unit after  
485 microalgae recovery, and may contain also some microalgae. NaOH mixing with microalgae and  
486 microbubbles in this system takes place directly in the injection system, and is different depending  
487 on its location on this injection system. For instance, in positions 3 and 6 (Figure 6a), mixing will be  
488 more efficient than in position 1 and 4 because there the flow rate is the most important and the  
489 fluid is already a tri-phase fluid (culture medium, cells and bubbles). Thus to find the best mixing  
490 conditions, we chose to inject NaOH at of 0.2 mol/L (final concentration of 0.02 mol/L in the  
491 microalgae suspension) at the different places in the injection system represented in red on the  
492 schematic representation in Figure 6a. After flocculation/flotation, the harvesting efficiencies were  
493 measured: results are presented in Figure 6b. They show that the best cell separation rates, of  
494 approximately 60%, are reached when NaOH is injected in the locations 3 and 6, where mixing is the  
495 most efficient. If NaOH is injected into the microalgae supply line, the harvesting performance is  
496 slightly higher if this injection is made at the outlet of the elbow (position 1), where recirculation  
497 phenomena occur because of the 90° bend located just upstream of position 1. However, these  
498 performances do not reach those achieved for a NaOH injection in the positions 3 and 6. On the  
499 pressurized water supply line, the further away the injection is from the confluence with the  
500 suspension feed, the lower the harvesting efficiency is. For instance, the harvesting efficiency is  
501 significantly reduced when NaOH is injected in the position 4; this can be explained by the low  
502 presence of microalgae in this pipe. The magnesium precipitate needs to be formed in the presence  
503 of the cells to best entrap them, thus explaining the lower separation efficiencies reached in the  
504 pressurized water supply line.

505           However in these experiments, the maximum harvesting efficiency obtained is of 60%. They  
506 were realized with a NaOH solution at a concentration of 0.2 mol/L: as showed before, best  
507 separation rates are obtained for diluted NaOH solutions, the best efficiencies being achieved in the

508 case of NaOH solutions of 0.1 mol/L (Figure 4c, 80% of cell separated from water). Thus, in order to  
509 optimize the NaOH concentration, using a NaOH injection in the position 3 in the injection system,  
510 the experiments were repeated with injected NaOH solutions of different concentrations (final NaOH  
511 concentration of 0.02 mol/L). The results are showed in Figure 7, where both the harvesting  
512 efficiencies obtained in batch-mode at laboratory scale and in continuous mode at pre-industrial  
513 scale are represented. It is clear on this graph that indeed, for a solution of NaOH of 0.1 mol/L, the  
514 separation rate reaches 80%, and decreases as the NaOH concentration increases. The interesting  
515 point is that for both harvesting modes (batch or continuous), the harvesting efficiencies are the  
516 same, thus showing the successful scale-up of our NaOH-induced flocculation/flotation process.  
517 Therefore, we could adapt an efficient injection system, allowing to separate in a single pass up to  
518 80% of the cells from their culture medium at high scale, and concentrate them by a factor of 230,  
519 compared to approximately 20 in laboratory-scale experiments. This difference in the concentration  
520 factor is explained by the fact that in the continuous DAF system, the rotation velocity of the  
521 scrapper, which removes floated microalgae, and its vertical position in the tank can be tuned in  
522 order to adapt the residence time of the foam containing the microalgae at the tank surface. During  
523 this residence, the microalgae concentration increases in the foam, due to the liquid drainage by  
524 gravity, resulting in higher concentration factors compared to lab-scaled experiments.

525

#### 526 **4. Conclusions**

527 We provide here an interdisciplinary multi-scale study to propose an efficient harvesting  
528 method for *D. salina* cells using flocculation/flotation, which can be used at industrial scales.  
529 Experiments at the nanoscale as well as simulations allowed first to precisely understand the  
530 complete mechanism of flocculation by addition of NaOH in the complex hypersaline medium in  
531 which *D. salina* grows. We thus brought strong scientific arguments proving that addition of NaOH in  
532 the medium creates a magnesium hydroxide precipitate that entraps the cell and flocculate them  
533 through sweeping. Because no other mechanism is involved, the formation of this precipitate, at low

534 speed, in the entire microalgae suspension, is determinant for the harvesting efficiency.  
535 Understanding this then led us to evaluate the influence of pertinent parameters to achieve high-  
536 efficiency harvesting, all related to the precipitation of  $Mg(OH)_2$ , that are the NaOH concentration in  
537 the medium, the agitation and the salinity of the medium. Our results, in laboratory-scale  
538 flocculation/flotation experiments, allowed us to show that the added NaOH solution had to be  
539 diluted, the agitation had to be optimal to bring the NaOH in the entire volume without breaking the  
540 forming flocs, and that too high salinities were resulting in magnesium hydroxide supersaturation  
541 phenomena. It is based on this understanding of the separation mechanisms and on the  
542 identification of the influence of different parameters on the harvesting performances that the  
543 transition of the process to the pre-industrial scale could be addressed from in an efficient way. For  
544 that we focused on the mixing efficiency at the injection site and the NaOH concentration injected to  
545 provide optimal parameters and achieve efficient microalgae harvesting at high-scale. Now further  
546 studies needs to be done to evaluate with precision the cost and energy consumption of this process  
547 at high-scale, and optimize better flocculation conditions to achieve effective harvesting at lower  
548 costs. Experiments have already been performed in this way, using slaked lime as a base to induce  
549 the precipitation of magnesium hydroxide. Our results so far show promising harvesting efficiencies,  
550 achieved at lower cost as calcite is less expensive than NaOH.

551

552

553 **Acknowledgements**

554 A. B. is a PhD student supported by the FUI Salinalgue. C. F.-D. is a postdoctoral researcher supported  
555 by the AgreenSkills fellowship programme, which has received funding from the EU's Seventh  
556 Framework Programme under grant agreement No. FP7-609398 (AgreenSkills+contract).

557

558 **Author contribution**

559 P. G. conceived the project. A. B. and C. F.-D. conceived and performed the experiments. P. G., A. B.  
560 and C. F.-D. discussed and interpreted the results. C. F.-D. and A. B. wrote the manuscript. P. G., A. B.,  
561 and C. F.-D. reviewed and contributed to the manuscript. All authors approved the final manuscript.

562

563



564 **References**

- 565 Ambati, R.R., Gogisetty, D., Aswathanarayana, R.G., Ravi, S., Bikkina, P.N., Bo, L., Yuepeng, S., 2018.  
566 Industrial potential of carotenoid pigments from microalgae: Current trends and future prospects.  
567 Crit. Rev. Food Sci. Nutr. 1–22. <https://doi.org/10.1080/10408398.2018.1432561>
- 568 Anila, N., Simon, D.P., Chandrashekar, A., Ravishankar, G.A., Sarada, R., 2016. Metabolic engineering  
569 of *Dunaliella salina* for production of ketocarotenoids. Photosynth. Res. 127, 321–333.  
570 <https://doi.org/10.1007/s11120-015-0188-8>
- 571 Baseggio, G., 1974. The composition of sea water and its concentrates, in: Proceedings of the Fourth  
572 Symposium on Salt, 8-12 April 1973. pp. 351–358.
- 573 Béchet, Q., Coulombier, N., Vasseur, C., Lasserre, T., Le Dean, L., Bernard, O., 2018. Full-scale  
574 validation of an algal productivity model including nitrogen limitation. Algal Res. 31, 377–386.  
575 <https://doi.org/10.1016/j.algal.2018.02.010>
- 576 Besson, A., 2013. Etude multi-échelle de la récolte de *Dunaliella salina*-Développement d'un procédé  
577 d'autofloculation-flottation de microalgues (PhD Thesis). Toulouse, INSA.
- 578 Besson, A., Guiraud, P., 2013. High-pH-induced flocculation-flotation of the hypersaline microalga  
579 *Dunaliella salina*. Bioresour. Technol. 147, 464–470. <https://doi.org/10.1016/j.biortech.2013.08.053>
- 580 Besson, A., Guiraud, P., 2012. Effects of pH adjustment on Dissolved Air Flotation harvesting of the  
581 hypersaline microalga *Dunaliella salina*., in: 6th International IWA Conference on Flotation for Water  
582 and Wastewater Systems. New-York city.
- 583 Binnig, G., Quate, C.F., Gerber, C., 1986. Atomic Force Microscope. Phys. Rev. Lett. 56, 930–934.
- 584 Bonnefond, H., Moelants, N., Talec, A., Mayzaud, P., Bernard, O., Sciandra, A., 2017. Coupling and  
585 uncoupling of triglyceride and beta-carotene production by *Dunaliella salina* under nitrogen  
586 limitation and starvation. Biotechnol. Biofuels 10, 25. <https://doi.org/10.1186/s13068-017-0713-4>
- 587 Branyikova, I., Filipenska, M., Urbanova, K., Ruzicka, M.C., Pivokonsky, M., Branyik, T., 2018.  
588 Physicochemical approach to alkaline flocculation of *Chlorella vulgaris* induced by calcium phosphate

589 precipitates. Colloids Surf. B Biointerfaces 166, 54–60.  
590 <https://doi.org/10.1016/j.colsurfb.2018.03.007>

591 Chen, H., Jiang, J.-G., 2009. Osmotic responses of *Dunaliella* to the changes of salinity. *J. Cell. Physiol.*  
592 219, 251–258. <https://doi.org/10.1002/jcp.21715>

593 Clift, R., Grace, J.R., Weber, M.E., Clift, R., 1978. Bubbles, drops, and particles. Academic press New  
594 York.

595 Debye, P., Hückel, E., 1923. The theory of electrolytes. I. Lowering of freezing point and related  
596 phenomena. *Phys. Z.* 24, 185–206.

597 Edzwald, J.K., 1995. Principles and applications of dissolved air flotation. *Water Sci. Technol.*,  
598 Flotation Processes in Water and Sludge Treatment 31, 1–23. [https://doi.org/10.1016/0273-](https://doi.org/10.1016/0273-1223(95)00200-7)  
599 [1223\(95\)00200-7](https://doi.org/10.1016/0273-1223(95)00200-7)

600 Feng, S., Li, X., Xu, Z., Qi, J., 2014. *Dunaliella salina* as a novel host for the production of recombinant  
601 proteins. *Appl. Microbiol. Biotechnol.* 98, 4293–4300. <https://doi.org/10.1007/s00253-014-5636-4>

602 Formosa-Dague, C., Gernigon, V., Castelain, M., Daboussi, F., Guiraud, P., 2018. Towards a better  
603 understanding of the flocculation/flotation mechanism of the marine microalgae *Phaeodactylum*  
604 *tricornutum* under increased pH using atomic force microscopy. *Algal Res.* 33, 369–378.  
605 <https://doi.org/10.1016/j.algal.2018.06.010>

606 Francius, G., Tesson, B., Dague, E., Martin-Jézéquel, V., Dufrêne, Y.F., 2008. Nanostructure and  
607 nanomechanics of live *Phaeodactylum tricornutum* morphotypes. *Environ. Microbiol.* 10, 1344–1356.  
608 <https://doi.org/10.1111/j.1462-2920.2007.01551.x>

609 Garg, S., Li, Y., Wang, L., Schenk, P.M., 2012. Flotation of marine microalgae: effect of algal  
610 hydrophobicity. *Bioresour. Technol.* 121, 471–474. <https://doi.org/10.1016/j.biortech.2012.06.111>

611 Garg, S., Wang, L., Schenk, P.M., 2015. Flotation separation of marine microalgae from aqueous  
612 medium. *Sep. Purif. Technol.* 156, 636–641. <https://doi.org/10.1016/j.seppur.2015.10.059>

613 Harvie, C.E., Møller, N., Weare, J.H., 1984. The prediction of mineral solubilities in natural waters:  
614 The Na-K-Mg-Ca-H-Cl-SO<sub>4</sub>-OH-HCO<sub>3</sub>-CO<sub>3</sub>-CO<sub>2</sub>-H<sub>2</sub>O system to high ionic strengths at 25°C. *Geochim.*  
615 *Cosmochim. Acta* 48, 723–751. [https://doi.org/10.1016/0016-7037\(84\)90098-X](https://doi.org/10.1016/0016-7037(84)90098-X)

616 Hutter, J.L., Bechhoefer, J., 1993. Calibration of atomic-force microscope tips. *Rev. Sci. Instrum.* 64,  
617 1868–1873.

618 Khadim, S.R., Singh, P., Singh, A.K., Tiwari, A., Mohanta, A., Asthana, R.K., 2018. Mass cultivation of  
619 *Dunaliella salina* in a flat plate photobioreactor and its effective harvesting. *Bioresour. Technol.* 270,  
620 20–29. <https://doi.org/10.1016/j.biortech.2018.08.071>

621 Kim, W., Park, J.M., Gim, G.H., Jeong, S.-H., Kang, C.M., Kim, D.-J., Kim, S.W., 2012. Optimization of  
622 culture conditions and comparison of biomass productivity of three green algae. *Bioprocess Biosyst.*  
623 *Eng.* 35, 19–27. <https://doi.org/10.1007/s00449-011-0612-1>

624 Lamers, P.P., Janssen, M., De Vos, R.C.H., Bino, R.J., Wijffels, R.H., 2012. Carotenoid and fatty acid  
625 metabolism in nitrogen-starved *Dunaliella salina*, a unicellular green microalga. *J. Biotechnol.* 162,  
626 21–27. <https://doi.org/10.1016/j.jbiotec.2012.04.018>

627 Lin, J.X., Wang, L., 2009. Adsorption of dyes using magnesium hydroxide-modified diatomite.  
628 *Desalination Water Treat.* 8, 263–271. <https://doi.org/10.5004/dwt.2009.786>

629 Metting, F.B., 1996. Biodiversity and application of microalgae. *J. Ind. Microbiol.* 17, 477–489.  
630 <https://doi.org/10.1007/BF01574779>

631 Minhas, A.K., Hodgson, P., Barrow, C.J., Adholeya, A., 2016. A Review on the Assessment of Stress  
632 Conditions for Simultaneous Production of Microalgal Lipids and Carotenoids. *Front. Microbiol.* 7.  
633 <https://doi.org/10.3389/fmicb.2016.00546>

634 Nguyen, T.D.P., Frappart, M., Jaouen, P., Pruvost, J., Bourseau, P., 2014. Harvesting *Chlorella vulgaris*  
635 by natural increase in pH: effect of medium composition. *Environ. Technol.* 35, 1378–1388.  
636 <https://doi.org/10.1080/09593330.2013.868531>

637 Oren, A., 2005. A hundred years of *Dunaliella* research: 1905–2005. *Saline Syst.* 1, 2.  
638 <https://doi.org/10.1186/1746-1448-1-2>

639 Oseen, C.W., 1910. Stokes' Formula and a Related Theorem in Hydrodynamics. *Ark. Mat Astron Fys.*  
640 6, 20.

641 Pirwitz, K., Rihko-Struckmann, L., Sundmacher, K., 2015. Comparison of flocculation methods for  
642 harvesting *Dunaliella*. *Bioresour. Technol.* 196, 145–152.  
643 <https://doi.org/10.1016/j.biortech.2015.07.032>

644 Pitzer, K.S., 1975. Thermodynamics of electrolytes. V. Effects of higher-order electrostatic terms. *J.*  
645 *Solut. Chem.* 4, 249–265.

646 Pitzer, K.S., 1973. Thermodynamics of electrolytes. I. Theoretical basis and general equations. *J. Phys.*  
647 *Chem.* 77, 268–277. <https://doi.org/10.1021/j100621a026>

648 Pitzer, K.S., Kim, J.J., 1974. Thermodynamics of electrolytes. IV. Activity and osmotic coefficients for  
649 mixed electrolytes. *J. Am. Chem. Soc.* 96, 5701–5707.

650 Pitzer, K.S., Mayorga, G., 1974. Thermodynamics of electrolytes. III. Activity and osmotic coefficients  
651 for 2–2 electrolytes. *J. Solut. Chem.* 3, 539–546.

652 Pitzer, K.S., Mayorga, G., 1973. Thermodynamics of electrolytes. II. Activity and osmotic coefficients  
653 for strong electrolytes with one or both ions univalent. *J. Phys. Chem.* 77, 2300–2308.

654 Pragma, N., Pandey, K.K., Sahoo, P.K., 2013. A review on harvesting, oil extraction and biofuels  
655 production technologies from microalgae. *Renew. Sustain. Energy Rev.* 24, 159–171.  
656 <https://doi.org/10.1016/j.rser.2013.03.034>

657 Prieto, A., Pedro Cañavate, J., García-González, M., 2011. Assessment of carotenoid production by  
658 *Dunaliella salina* in different culture systems and operation regimes. *J. Biotechnol.* 151, 180–185.  
659 <https://doi.org/10.1016/j.jbiotec.2010.11.011>

660 Srinivasan, R., Chaitanyakumar, A., Mageswari, A., Gomathi, A., Pavan Kumar, J.G.S., Jayasindu, M.,  
661 Bharath, G., Shravan, J.S., Gothandam, K.M., 2017. Oral administration of lyophilized *Dunaliella*  
662 *salina*, a carotenoid-rich marine alga, reduces tumor progression in mammary cancer induced rats.  
663 *Food Funct.* 8, 4517–4527. <https://doi.org/10.1039/c7fo01328k>

664 Sukenik, A., Shelef, G., 1984. Algal autoflocculation--verification and proposed mechanism.  
665 Biotechnol. Bioeng. 26, 142–147. <https://doi.org/10.1002/bit.260260206>

666 Uduman, N., Qi, Y., Danquah, M.K., Forde, G.M., Hoadley, A., 2010. Dewatering of microalgal  
667 cultures: A major bottleneck to algae-based fuels. J. Renew. Sustain. Energy 2, 012701.  
668 <https://doi.org/10.1063/1.3294480>

669 Vandamme, D., Foubert, I., Fraeye, I., Meesschaert, B., Muylaert, K., 2012. Flocculation of *Chlorella*  
670 *vulgaris* induced by high pH: Role of magnesium and calcium and practical implications. Bioresour.  
671 Technol. 105, 114–119. <https://doi.org/10.1016/j.biortech.2011.11.105>

672 Vandamme, D., Foubert, I., Muylaert, K., 2013. Flocculation as a low-cost method for harvesting  
673 microalgae for bulk biomass production. Trends Biotechnol. 31, 233–239.  
674 <https://doi.org/10.1016/j.tibtech.2012.12.005>

675 Vandamme, D., Pohl, P.I., Beuckels, A., Foubert, I., Brady, P.V., Hewson, J.C., Muylaert, K., 2015.  
676 Alkaline flocculation of *Phaeodactylum tricornutum* induced by brucite and calcite. Bioresour.  
677 Technol. 196, 656–661. <https://doi.org/10.1016/j.biortech.2015.08.042>

678 Walne, P.R., 1970. Studies on the food value of nineteen genera of algae to juvenile bivalves of the  
679 genera *Ostrea*, *Crassostrea*, *Mercenaria* and *Mytilus*. Fish. Invest Lond 5, 62.

680 Wu, Z., Zhu, Y., Huang, W., Zhang, C., Li, T., Zhang, Y., Li, A., 2012. Evaluation of flocculation induced  
681 by pH increase for harvesting microalgae and reuse of flocculated medium. Bioresour. Technol. 110,  
682 496–502. <https://doi.org/10.1016/j.biortech.2012.01.101>

683 Xiong, Q., Pang, Q., Pan, X., Chika, A.O., Wang, L., Shi, J., Jia, L., Chen, C., Gao, Y., 2015. Facile sand  
684 enhanced electro-flocculation for cost-efficient harvesting of *Dunaliella salina*. Bioresour. Technol.  
685 187, 326–330. <https://doi.org/10.1016/j.biortech.2015.03.135>

686 Yang, C., Dabros, T., Li, D., Czarnecki, J., Masliyah, J.H., 2001. Measurement of the Zeta Potential of  
687 Gas Bubbles in Aqueous Solutions by Microelectrophoresis Method. J. Colloid Interface Sci. 243, 128–  
688 135. <https://doi.org/10.1006/jcis.2001.7842>

689

690 **Figure captions**

691 **Figure 1. Schematic representation of the dissolved air flotation devices used.** (a) DAF device used  
692 at the laboratory-scale and (b) at the pre-industrial scale (with the courtesy of Serinol). In (b), the  
693 position of the NaOH line and needle valve depend on the injection site chosen to perform the  
694 experiment.

695

696 **Figure 2. Simulating the influence of the addition of NaOH on the ionic equilibria in *D. salina***  
697 **culture medium.** Phreeqc simulation of the pH and precipitates formation upon addition of NaOH in  
698 the culture medium.

699

700 **Figure 3. Probing the interactions between *D. salina* cells and magnesium hydroxides.** (a) Histogram  
701 representing the adhesion force distribution recorded on cells in sorbitol buffer at pH = 10 with bare  
702 AFM tips, and (b) histogram representing the rupture distance distributions in these conditions. The  
703 inset in (a) is an optical image of a *D. salina* cell and of the AFM probe; the inset in (b) shows  
704 representative retract force curves obtained. (c) Histogram representing the adhesion force  
705 distribution recorded on cells in sorbitol buffer at pH = 10 with Mg(OH)<sub>2</sub> functionalized AFM tips, and  
706 (d) histogram representing the rupture distance distributions in these conditions. Inset in (d) shows  
707 representative retract force curves obtained.

708

709 **Figure 4. Influence of the NaOH injection way on the harvesting efficiencies.** (a) Scheme  
710 representing the principle of the two injection systems used. In each case, the same quantity of  
711 NaOH is added, and the same final NaOH concentration in the microalgae suspension is reached. (b)  
712 Flocculation/flotation harvesting efficiencies obtained for a final NaOH concentration of 0.02 mol/L  
713 using the direct injection system (open symbols) or the diluted injection system (black-filled symbols)  
714 and in both case a NaOH solution of 1 mol/L. (c) Flocculation/flotation harvesting efficiencies

715 obtained for a final NaOH concentration of 0.02 mol/L using the diluted injection system and injected  
716 NaOH solutions of different concentrations.

717 **Figure 5. Influence of agitation and salinity on the harvesting efficiencies.** (a) Influence of the  
718 agitation speed on the harvesting efficiency obtained for a final NaOH concentration of 0.02 mol/L  
719 using the diluted injection system with a NaOH solution of 1 mol/L. Open diamonds symbols  
720 correspond to an agitation speed of 20 rpm, black-filled circles correspond to 40 rpm, and black-filled  
721 diamonds correspond to 80 rpm. (b) Influence of the salinity of the culture medium on the  
722 harvesting efficiency obtained for a final NaOH concentration of 0.02 mol/L using the diluted  
723 injection system with a NaOH solution of 1 mol/L. Cross symbols correspond to a salinity of 7.5%,  
724 open-squares correspond to a salinity of 12% and open-circles correspond to a salinity of 15.2%.

725

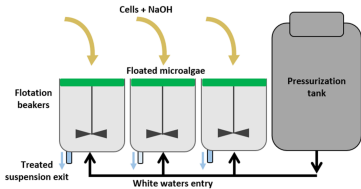
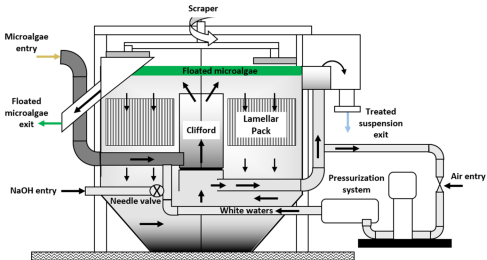
726 **Figure 6. Adaptation of the NaOH injection system for high-scale harvesting.** (a) Schematic and  
727 simplified representation of the injection system of the microalgae suspension and of the pressurized  
728 water into the industrial flotation unit. Red crosses represents the positions on the injection system  
729 where NaOH can be injected. The waters sued for pressurization are recycled from the flotation unit  
730 after cell recovery and may contain some microalgae. (b) Influence of the NaOH injection position on  
731 the flocculation/flotation harvesting efficiency obtained for a final NaOH concentration of 0.02 mol/L  
732 and a NaOH solution of 0.2 mol/L.

733

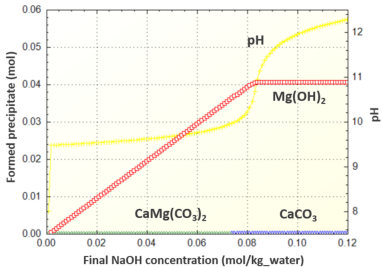
734 **Figure 7. Influence of the injected NaOH concentration on the harvesting efficiency.**  
735 Flocculation/flotation harvesting efficiencies obtained for a final NaOH concentration of 0.02 mol/L  
736 injected NaOH solutions of different concentrations. Results obtained in batch mode using diluted  
737 injection (open diamond symbols) or in continuous mode with NaOH injection in position 3  
738 represented in Figure 5a (black-filled diamond symbols).

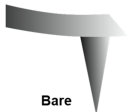
739

740

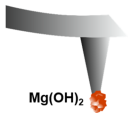
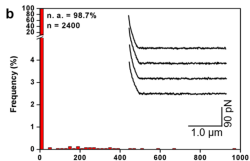
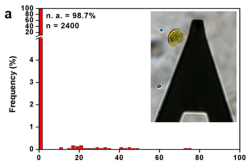
**a****b**



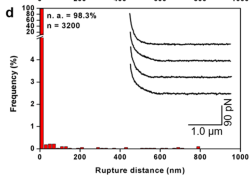
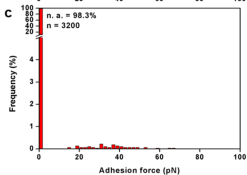


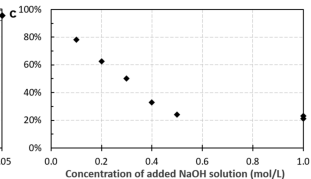
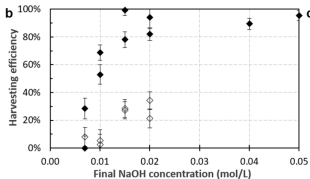
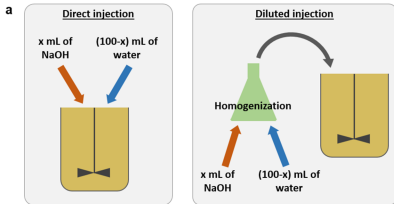


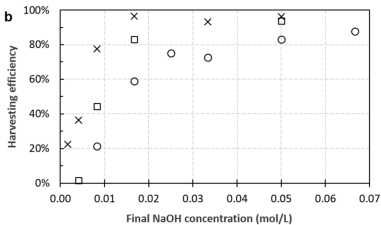
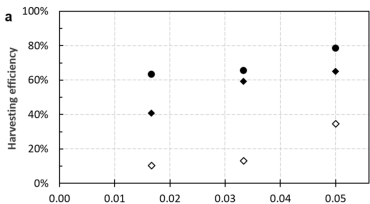
Bare

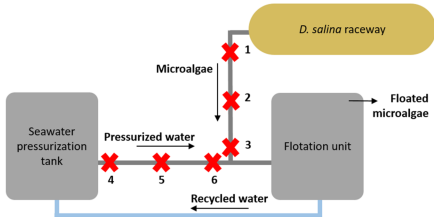
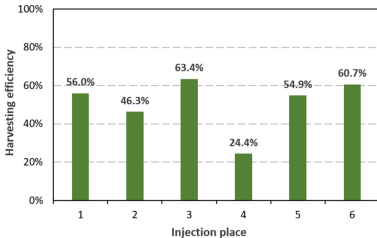


Mg(OH)<sub>2</sub>







**a****b**

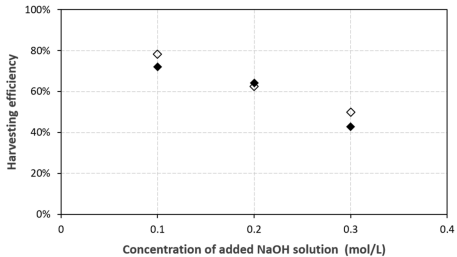
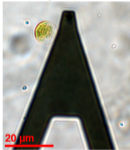


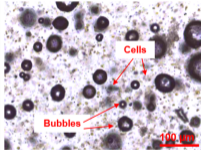
**Table 1.** Concentrations of the main ions in the culture medium used in g/L

Na <sup>+</sup>	Cl <sup>-</sup>	SO <sub>4</sub> <sup>2-</sup>	Mg <sup>2+</sup>	Ca <sup>2+</sup>	K <sup>+</sup>
42.12	67.08	1.87	0.95	0.39	0.04

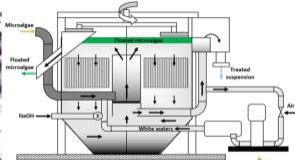
AFM to probe *D. salina* interactions with  $Mg(OH)_2$  particles



Sweeping of cells and microbubbles during  $Mg(OH)_2$  precipitation



Industrial harvesting of *D. salina* by flocculation/flotation



Molecular scale

Pre-industrial scale